TPM Vol. 32, No. S9, 2025
ISSN: 1972-6325
https://www.tpmap.org/

BRIDGING DEPTH AND BREADTH: A WIDE–DEEP CUSTOM NEURAL NETWORK FOR ENHANCED COVID-19 DETECTION FROM CT-SCAN IMAGES

PARASHURAM BANNIGIDAD[1], VAISHALI KALE[2]

[1] DEPARTMENT OF COMPUTER SCIENCE, RANI CHANNAMMA UNIVERSITY, BELAGAVI-591156, KARNATAKA, INDIA. EMAIL: parashurambannigidad@gmail.com, ORCID: 0000-0001-6191-6117
[2] RESEARCH SCHOLAR, DEPARTMENT OF COMPUTER SCIENCE, RANI CHANNAMMA UNIVERSITY, BELAGAVI-591156, KARNATAKA, INDIA. EMAIL: vrajarani.rns@gmail.com, ORCID:0000-0001-7916-4160

Abstract. Coronavirus Disease 2019 (COVID-19) continues to pose a significant global health threat, necessitating accurate and efficient diagnostic methods. Manual analysis of CT scans is time-consuming and susceptible to errors, emphasizing the need for automated diagnostic tools. This paper presents a novel Custom Wide and Deep Neural Network (WDNN) developed from scratch for the binary classification of COVID-19 and non-COVID CT-scan images. Unlike conventional approaches that leverage transfer learning with pre-trained models such as VGG19, ResNet50, and InceptionV3, our architecture is fully data-driven and domain-specific. The model integrates a dual-branch structure combining a wide input layer and a deep convolutional path enhanced by a custom ExpandDimLayer. Real-time data augmentation techniques and grayscale preprocessing were employed to improve robustness and generalization. Evaluations were conducted on a comprehensive dataset of 15,000 2D CT-scan slices sourced from Kaggle public repository and Lakeview Hospital, Belagavi, organized into COVID and non-COVID categories. The proposed Custom-built Wide and Deep Neural Network model achieved exceptional performance with 99.49% accuracy, 99.31% precision, 99.68% recall, and 99.47% F1-score through rigorous 5-fold cross-validation, significantly outperforming existing transfer learning-based models. The model includes real-time prediction capabilities with Grad-CAM visualization for improved clinical interpretability. These results confirm the effectiveness of custom-built deep learning architectures for COVID-19 detection and broader medical imaging applications.

Keywords: COVID-19, CT-scan classification, Wide and Deep Neural Network (WDNN), deep learning, medical image analysis, automatic diagnosis, binary classification, data augmentation.

INTRODUCTION

COVID-19, triggered by the SARS-CoV-2 virus, has significantly altered global diagnostic and healthcare practices [1]. Timely and precise diagnosis is essential for effective disease management. CT scans have become a key diagnostic tool due to their high sensitivity in detecting hallmark lung features of COVID-19, including ground-glass opacities and bilateral consolidations, even in early or asymptomatic stages[2][3].Despite the critical role of radiologists, manual CT analysis is challenged by time pressure, inter-observer variability, and diagnostic errors, issues worsened by the surge in imaging data during the pandemic[4]. Consequently, automated diagnostic tools leveraging artificial intelligence are increasingly necessary to augment clinical decision-making and improve diagnostic efficiency[5].

Deep learning has demonstrated substantial promise in medical image analysis, particularly for COVID-19 detection[6]. The existing literature commonly utilizes convolutional neural networks pretrained on ImageNet and fine tunes them for COVID-19 detection in CT scans. This strategy simplifies training with limited datasets but constrains the network's ability to learn richer domain specific features. Among these, several architectures have gained prominence in COVID-19 diagnosis from CT scans. Simonyan and Zisserman [7] introduced VGG19, a deep convolutional architecture with 19 layers featuring small 3×3 filters, which has been widely adopted for medical image classification. K. He et al. [8] proposed ResNet50, incorporating residual connections to enable training of deeper networks while mitigating gradient vanishing problems. Szegedy et al. [9] developed InceptionV3, employing multi-scale convolutional filters through inception modules to capture features at different spatial resolutions. These architectures have been extensively applied to COVID-19 detection, with Sahinbas K et al. [10] reporting accuracies up to 80% using transfer learning-based convolutional neural network for COVID-19 detection with X-ray images. Chouat et al. [11] used deep transfer learning by evaluating several pre-trained convolutional neural network architectures (VGG-19, ResNet50, InceptionV3, and Xception) for automatic classification of COVID-19 from both CT-scan and chest X-ray (CXR) images. Foysal Md et al. [12]proposed the use of deformable convolutional neural networks for COVID-19 screening from chest CT images, converting both a standard CNN and a ResNet-50 model into deformable-CNN versions to detect infection. Their work highlights the benefit of deformable convolutional architectures for medical imaging tasks,

offering enhanced adaptability in sampling spatial features compared with conventional CNNs when applied directly on CT data for COVID-19 classification. Sahithya N. et al. [13]applied the deep convolutional neural network VGG-19, fine-tuned on chest CT-scan images, to classify cases as COVID-19 or normal. Gunraj et al. [14] introduced COVID-Net CT-2, a deep learning model specifically designed for COVID-19 detection from chest CT images, built using a larger and more diverse training strategy to improve representation of real-world variability. Ko et al. [4] developed a 2D deep learning framework utilizing transfer learning for COVID-19 diagnosis via chest CT, demonstrating the feasibility of adapting ImageNet-trained models to medical imaging. Zhang et al. [14] proposed an automated system for detecting and quantifying COVID-19 pneumonia in CT-scan images using modified ResNet architectures. Huang M. et al. [15] recently introduced a LightEfficientNetV2 model for COVID-19 and pneumonia classification, achieving competitive performance with an accuracy of 97.48% on CT-scan images. Ismael A. et al. [16] employed deep-learning strategies, including pretrained CNN feature extraction, fine-tuning, and a newly developed end-to-end CNN to classify COVID-19 from chest X-ray images, achieving the highest accuracy with ResNet50 features combined with a linear SVM classifier. Despite achieving high accuracies, transfer learning approaches face inherent limitations when applied to medical imaging. The fundamental mismatch between natural images and medical images results in suboptimal feature representations, as features learned from everyday objects poorly align with pathological patterns in CT scans [17]. Wang et al. [18] highlighted this challenge, proposing contrastive learning to better adapt features for radiography images. Furthermore, pre-trained models often require extensive fine-tuning and may still retain biases toward natural image characteristics, potentially limiting their effectiveness in capturing domain-specific medical features [10].

Recent work has explored training models from scratch for medical imaging applications. Khan et al. [20] introduced a two-phase framework that includes the SB STM BRNet CNN for COVID-19 detection from CT images and the COVID CB RESeg CNN for infection segmentation, both designed to learn domain-specific features more effectively than models adapted from natural image tasks. Recent comprehensive reviews have further validated this trend, with Takahashi et al. [19] conducting systematic comparisons between Vision Transformers and CNNs in medical image analysis, demonstrating that architecture selection significantly impacts diagnostic performance across different imaging modalities. Azad et al. [20] provided an extensive review of advances in medical image analysis with Vision Transformers, highlighting the importance of domain-specific architectural innovations. Halder et al. [21] successfully implemented Vision Transformers for classifying 2D biomedical images, demonstrating the viability of attention-based mechanisms in medical contexts. Hiremath and Bannigidad [22] demonstrated the effectiveness of custom image processing algorithms for automated classification of biomedical images, showing that domain-specific feature extraction can outperform generic approaches in medical applications. Furthermore, ensemble approaches combining multiple architectures have shown promise, with Sedik et al. [23] deploying augmented data strategies to improve model robustness. These findings motivate the development of custom architectures explicitly designed for medical image characteristics rather than relying on feature transfer from unrelated domains.

The importance of model interpretability in clinical settings has also gained significant attention. Explainable AI techniques, particularly Gradient-weighted Class Activation Mapping (Grad-CAM), have emerged as essential tools for building clinical trust in automated diagnostic systems [24]. Recent studies have demonstrated the efficacy of Grad-CAM in medical imaging applications, with Suara et al. [25] showing its effectiveness in identifying diagnostically relevant regions in chest X-rays for COVID-19 detection, and M et al. [24] successfully applying Grad-CAM with ResNet50 for brain tumor detection in MRI images. These visualization techniques enable clinicians to verify that model predictions are based on clinically relevant features rather than spurious correlations or artifacts [25].

Existing transfer learning approaches have demonstrated encouraging outcomes, yet their reliance on pretrained weights derived from natural image domains limits their ability to fully capture the complex intensity patterns and structural variations present in medical imaging. To bridge this methodological gap, we introduce a custom Wide and Deep Neural Network trained entirely from scratch for COVID 19 CT-scan classification. This domain specific architecture is designed to learn modality aware representations directly from the data, thereby addressing the feature-learning constraints commonly associated with transfer learning-based models. The proposed work introduces a novel Wide and Deep Neural Network (WDNN) architecture specifically designed for the binary classification of COVID-19 CT images, developed entirely from scratch to overcome the domain mismatch limitations of transfer learning. The model integrates a dual-branch framework that combines wide and deep feature extraction paths, enhanced by a custom ExpandDimLayer, which enables the simultaneous capture of memorization-based and generalization-based patterns within medical images. Through extensive experimentation, the study provides empirical evidence that custom-built architectures trained from scratch can outperform well-established transfer learning models such as VGG19, ResNet50, and InceptionV3 in medical imaging tasks. Furthermore, rigorous validation performed on a dataset of 15,000 2D CT-scan slices using 5-fold cross-validation demonstrates superior performance, achieving 99.49% accuracy, 99.31% precision, 99.68% recall, and 99.47% F1-score, along with enhanced interpretability through Grad-CAM visualization.

MATERIALS AND METHODS

The dataset employed in this study comprises 15,000 2D CT-scan slices, collected from two primary sources to ensure diversity and clinical relevance. The first source includes anonymized clinical CT data from Lakeview Hospital, Belagavi, obtained in compliance with ethical and data privacy regulations. The second source consists of publicly available COVID-19 CT-scan datasets from the Kaggle platform, incorporated to enhance variability and improve generalization. The combined dataset covers both COVID-positive and non-COVID cases (including normal and pneumonia-affected lungs) with balanced representation to minimize class bias during training. This configuration enables robust model learning and fair evaluation. Experimental implementation was carried out on a Windows workstation equipped with an Intel Core i5-1135G7 CPU and 8 GB RAM, using Python 3.9 under the Anaconda environment with Jupyter Notebook as the primary development interface.

PROPOSED METHOD

The proposed Custom Wide and Deep Neural Network (WDNN) represents a novel approach for COVID-19 detection from CT-scan slices. The framework comprises three integrated stages: (i) Preprocessing, (ii) Data Augmentation, and (iii) Classification with WDNN. Figure 1, given below, depicts the flow diagram of the proposed method.

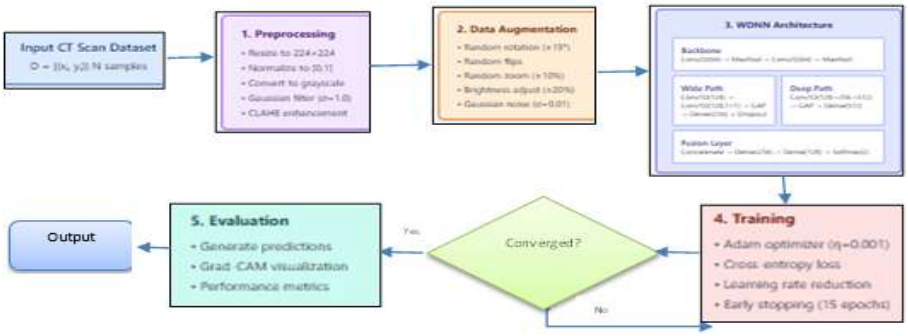

Figure 1. Flow diagram of the proposed method

Proposed Algorithm*:* Custom-Built Wide and Deep Neural Network (WDNN) for COVID-19 Detection

1) **Preprocessing:** Resize images to 224×224, normalize to [0,1], convert to grayscale, and apply Gaussian filtering (σ=1.0) and CLAHE (clip=2.0, tiles=8×8).

2) **Data Augmentation:** Apply random rotations (±15°), flips, zoom (±10%), brightness adjustment (±20%), and Gaussian noise (σ=0.01) with probability 0.5.

3) Architecture:

- *Backbone:* Two Conv2D layers (64 filters, 3×3 kernel) with MaxPooling
- *Wide Path:* Conv1D (128 filters) → Conv1D (128, 1×1) → GlobalAvgPool → Dense(256) + Dropout(0.5)
- *Deep Path:* Three Conv1D layers (128→256→512 filters) → GlobalAvgPool → Dense(512)
- *Fusion:* Concatenate paths → Dense(256) → Dense(128) → Softmax(2)

4) **Training:** Initialize with the normal weights. Train using the Adam optimizer (β_1=0.9, β_2=0.999) with categorical cross-entropy loss. Apply learning rate reduction (×0.5) after 5 epochs without validation improvement and early stopping after 15 epochs.

5) **Evaluation:** Generate predictions and Grad-CAM visualizations for test images.

Input: CT-scan dataset $D = \{(x_i, y_i)\}_{i=1}^{N}$, where $x_i \in R^{(H\times W\times C)}$, $y_i \in$ {COVID, Non-COVID}
Output: Trained model θ^*, predictions $\hat{y}$
Parameters: $\eta = 0.001$, batch size = 32, epochs = 100, dropout = 0.3-0.5

1.1 Preprocessing and Data Augmentation

All CT-scan slices were preprocessed to ensure uniformity, noise reduction, and improved feature visibility before model training. Each image was resized to 224×224 pixels, converted to grayscale to reduce computational load, and normalized to the [0, 1] range. Gaussian filtering (3×3 kernel, $\sigma = 1.0$) was applied to suppress acquisition noise, while Contrast Limited Adaptive Histogram Equalization (CLAHE; clip limit = 2.0, tile grid = 8×8) enhanced local contrast, improving the visibility of subtle COVID-19-related patterns such as ground-glass opacities and consolidations.

To improve generalization and prevent overfitting, real-time data augmentation was performed during training. Augmentation included random rotations (±15°), horizontal and vertical flips, zoom variations (±10%), brightness and contrast adjustments (±20%), translations, and Gaussian noise injection ($\sigma = 0.01$), thereby simulating diverse imaging conditions across scanners. These transformations were applied only to the training set, ensuring unbiased performance evaluation on validation and test data.

1.2 Classification with the Proposed WDNN Model

The proposed Custom Wide and Deep Neural Network (WDNN) was specifically designed for binary classification of COVID-19 and non-COVID CT-scan images. The model combines the strengths of wide and deep learning paradigms within a unified dual-branch framework to capture both broad intensity patterns and fine-grained spatial details.

3.2.1 Architecture Overview: The architecture comprises four integrated components: (i) Data Preparation, (ii) Custom Model Construction, (iii) Feature Learning, and (iv) Classification and Optimization, as shown in Figure 2a), given below.

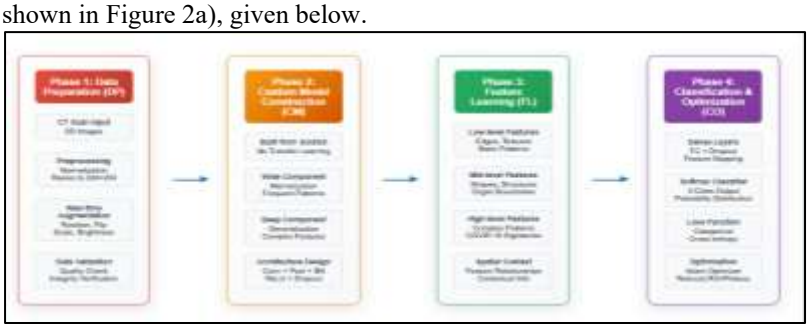

Figure 2. a) Architecture Overview of WDNN Model

The proposed WDNN model follows a dual-branch design that combines the strengths of wide and deep learning. The detailed architecture of the Wide and Deep neural network is depicted in Figure 2 b) given below.

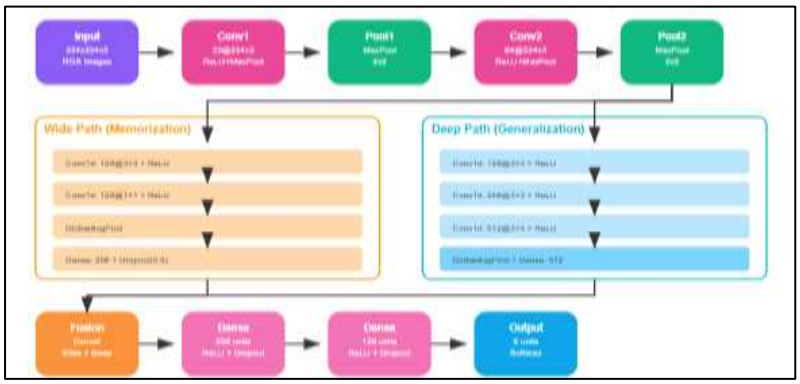

Figure 2. b) Wide and Deep Neural Network (WDNN) Detailed Architecture

The network starts with two convolutional layers (64 filters, 3×3 kernels, ReLU activation, and 2×2 max-pooling) that extract important spatial features from CT images. From this point, the model splits into two paths. The wide branch focuses on capturing global, intensity-based features across the image using convolutional and dense layers, which help the model remember key patterns related to COVID-19. The deep branch processes features through several convolutional layers with increasing filter depth (128 to 512), allowing it to learn more detailed and complex structures. A custom ExpandDimLayer increases the dimensional richness of features before both branches are combined in a fusion layer. Finally, the fused features pass through fully connected layers (256 and 128 neurons with dropout regularization) and a Softmax output layer to classify images as COVID or non-COVID.

3.2.2 Training Strategy and Optimization: The proposed WDNN was trained end-to-end from randomly initialized weights, enabling direct learning of domain-specific features from CT images rather than relying on pre-trained models. Training employed categorical cross-entropy loss with an adaptive learning rate regulated by the ReduceLROnPlateau callback to ensure efficient convergence and prevent overfitting. A 5-fold cross-validation protocol was implemented to guarantee unbiased and reliable evaluation across data partitions. Throughout 100 training epochs, the model exhibited smooth convergence with stable validation performance, supported by L2 regularization, batch normalization, dropout, and real-time data augmentation. The final model achieved a mean validation accuracy of 99.49%, reflecting excellent generalization capability and strong potential for clinical diagnostic applications.

1.3 Performance Evaluation Metrics

A comprehensive performance assessment was conducted using multiple evaluation metrics to ensure robust validation. The primary metrics include accuracy, precision, recall (sensitivity), and F1-score, calculated from the confusion matrix components: true positives (TP), true negatives (TN), false positives (FP), and false negatives (FN). These metrics provide comprehensive insight into model performance across different aspects of classification accuracy, ensuring clinical reliability and diagnostic confidence.

Accuracy: This metric measures the overall correctness of the model by calculating the ratio of correctly classified samples to the total number of samples, as shown in equation (1).

$$\text{Accuracy} = (TP + TN) / (TP + TN + FP + FN) \quad (1)$$

Precision: Precision quantifies the model's ability to avoid false alarms by measuring the proportion of positive predictions that are actually correct, as shown in equation (2).

$$\text{Precision} = TP / (TP + FP) \quad (2)$$

Recall: Recall evaluates the model's capability to identify all positive cases by calculating the proportion of actual positive cases that are correctly detected, as shown in equation (3).

$$\text{Recall} = TP / (TP + FN) \quad (3)$$

F1-Score: The F1-score provides a harmonic mean of precision and recall, offering a balanced measure that considers both false positives and false negatives, as shown in equation (4).

$$\text{F1-Score} = 2TP / (2TP + FP + FN) \quad (4)$$

EXPERIMENTAL RESULTS AND DISCUSSION

1.4 Training and Validation Performance

The proposed Custom Wide and Deep Neural Network (WDNN) was trained for 100 epochs under rigorous 5-fold cross-validation, ensuring consistent and unbiased model evaluation. Real-time data augmentation was applied throughout training to improve generalization and mitigate overfitting. The WDNN exhibited stable convergence, maintaining steadily increasing training and validation accuracy across all folds. Unlike transfer learning baselines, InceptionV3 (epoch 72), ResNet50 (epoch 68), and VGG19 (epoch 80), the proposed model continued improving until the final epoch, demonstrating its enhanced capacity for progressive feature refinement. Minimal divergence between training and validation curves confirmed strong regularization, achieved through the integration of L2 weight decay, batch normalization, dropout, and data augmentation strategies.

1.5 Overall Performance Metrics

The proposed WDNN model demonstrated exceptional performance across a comprehensive dataset comprising 15,000 CT-scan slices, evenly distributed between 7,500 COVID-positive and 7,500 non-COVID cases. The model achieved a remarkable overall accuracy of 99.49%, successfully classifying 14,924 out of 15,000 images with 7,476 true positives, 7,448 true negatives, 52 false positives, and 24 false negatives. The comprehensive performance metrics, as detailed in Table 1, revealed a precision of 99.31%, recall (sensitivity) of 99.68%, F1-score of 99.47%, specificity of 99.31%, AUC-ROC of 0.995, and Matthews Correlation Coefficient of 0.99. The model exhibited a total error count of 76 cases, translating to a minimal error rate of 0.51%. Notably, the exceptionally high recall of 99.68% demonstrates that merely 24 COVID-positive slices were misclassified. It is a crucial attribute for clinical screening applications where false negatives pose substantial clinical risk. Concurrently, the high precision of 99.31% ensures that false alarms remain minimal, thereby reducing unnecessary follow-up diagnostic procedures. Table 1 contains the full numeric summary.

Table 1. Performance metrics of the proposed WDNN model.

Metric	Value (%)	Confusion Matrix Element	Count
Accuracy	99.497	True Positives (TP)	7,476
Precision	99.310	True Negatives (TN)	7,448
Recall	99.687	False Positives (FP)	52
F1-Score	99.470	False Negatives (FN)	24
Specificity	99.317	Total Errors	76
AUC–ROC	99.5	Error Rate (%)	0.51
MCC	99.0	—	—

Figure 3(a), given below, shows the confusion matrix for InceptionV3, which exhibits moderate diagonal concentration, indicating reasonable classification accuracy; however, the presence of notable false positives and false negatives reveals limitations in distinguishing between COVID-positive and non-COVID CT-scan slices. Figure 3(b) presents the confusion matrix for ResNet50, demonstrating similarly moderate diagonal alignment with observable misclassifications, suggesting that while the model achieves acceptable performance, it still produces a considerable number of false positives and false negatives in the dataset. Figure 3(c) illustrates the confusion matrix for VGG19, which achieves notably stronger diagonal alignment compared to InceptionV3 and ResNet50, indicating improved feature discrimination capabilities; nevertheless, minor off-diagonal values persist, reflecting inherent limitations in transfer learning feature generalization for this specific medical imaging task. Figure 3(d) displays the confusion matrix for the proposed WDNN, revealing an almost perfectly diagonal structure with minimal off-diagonal entries—only 52 false positives and 24 false negatives—thereby confirming the model's outstanding accuracy of 99.49%, exceptional sensitivity of 99.68%, and high precision of 99.31%. This superior performance reinforces the effectiveness of the custom dual-branch architecture combined with the

domain-specific training strategy, which together enable superior feature extraction and deliver reliable clinical classification performance for COVID-19 detection from CT-scan images.

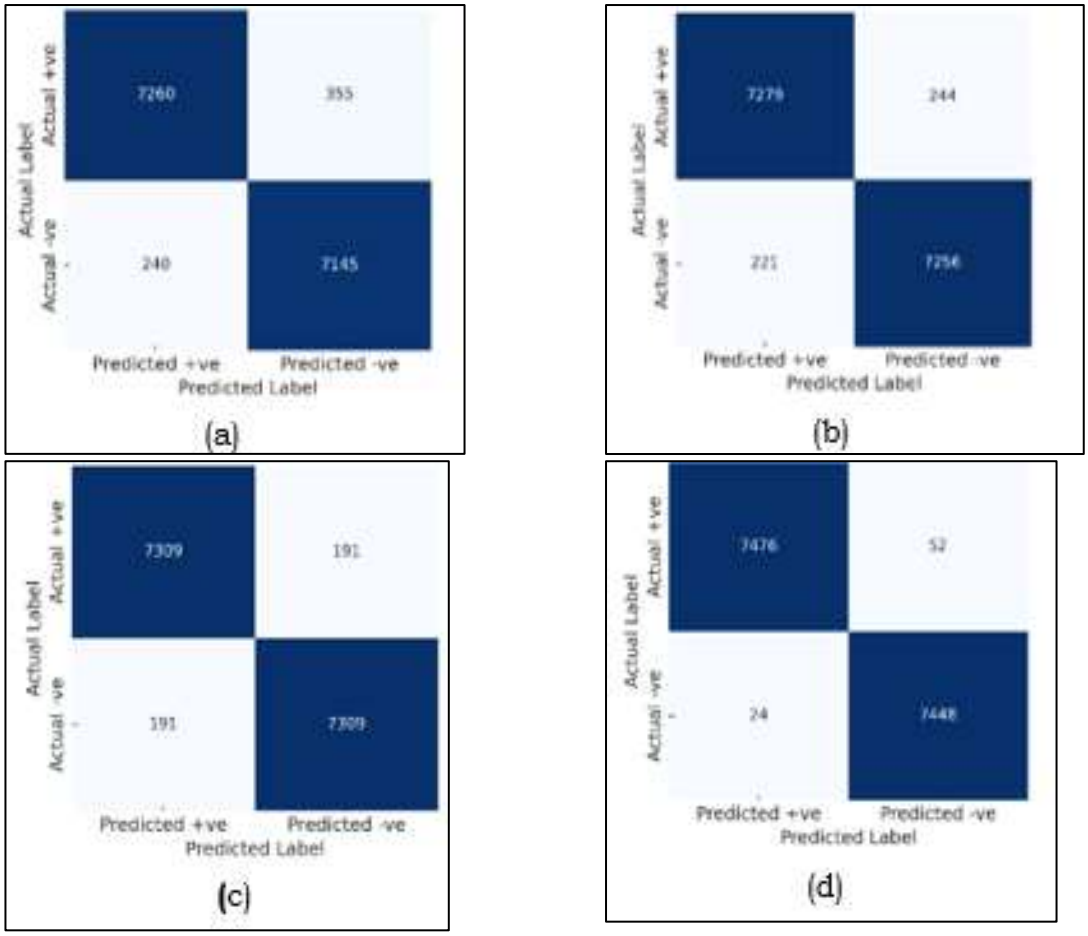

Figure 3. Confusion matrices illustrating classification performance of all models: (a) InceptionV3, (b) ResNet50, (c) VGG19, and (d) Proposed WDNN.

1.6 Cross-Validation Analysis

Performance consistency was evaluated through 5-fold cross-validation with carefully balanced folds, where each fold contained 3,000 slices equally distributed between 1,500 COVID-positive and 1,500 Non-COVID cases. Table 2 presents the fold-wise confusion matrix counts for both the proposed WDNN and the three transfer learning baseline models.

The WDNN demonstrated fold accuracies within a remarkably narrow range of 99.43% to 99.53%, achieving a mean accuracy of 99.49% with a standard deviation of ±0.20%. This tight clustering indicates excellent stability across different data partitions. In comparison, the baseline models exhibited substantially larger variability, with standard deviations of ±0.80% for InceptionV3, ±0.60% for ResNet50, and ±0.50% for VGG19, suggesting greater sensitivity to variations in dataset composition. These findings demonstrate the robust generalization capability of the WDNN across diverse data splits.

Table 2. Fold-wise confusion matrix results from 5-fold cross-validation.

Fold	Model	COVID +ve Correctly Detected (TP)	COVID +ve Wrongly Detected (FP)	COVID -ve Correctly Detected (TN)	COVID -ve Wrongly Detected (FN)	Fold Accuracy (%)
1	InceptionV3	1452	71	1429	48	96.03
1	ResNet50	1456	49	1451	44	96.90
1	VGG19	1462	38	1462	38	97.47
1	**Proposed Method**	**1495**	**10**	**1490**	**5**	**99.50**
2	InceptionV3	1440	75	1425	60	95.50
2	ResNet50	1459	47	1453	41	97.07
2	VGG19	1461	39	1461	39	97.40
2	**Proposed Method**	**1495**	**11**	**1489**	**5**	**99.47**
3	InceptionV3	1458	72	1428	42	96.20

3	ResNet50	1454	50	1450	46	96.80
3	VGG19	1463	37	1463	37	97.53
3	**Proposed Method**	**1496**	**10**	**1490**	**4**	**99.53**
4	InceptionV3	1464	65	1435	36	96.63
4	ResNet50	1453	48	1452	47	96.83
4	VGG19	1460	40	1460	40	97.33
4	**Proposed Method**	**1494**	**11**	**1489**	**6**	**99.43**
5	InceptionV3	1446	72	1428	54	95.80
5	ResNet50	1457	50	1450	43	96.90
5	VGG19	1463	37	1463	37	97.53
5	**Proposed Method**	**1496**	**10**	**1490**	**4**	**99.53**
TOTAL	InceptionV3	7,260	355	7,145	240	96.03
TOTAL	ResNet50	7,279	244	7,256	221	96.90
TOTAL	VGG19	7,309	191	7,309	191	97.35
TOTAL	**Proposed Method**	**7,476**	**52**	**7,448**	**24**	**99.49**

1.7 Comparative Analysis with Baseline Models

A comprehensive performance evaluation was conducted to compare the proposed Wide and Deep Neural Network architecture against three established baseline models, viz. InceptionV3, ResNet50, and VGG19, as shown in Table 3. The baseline models achieved accuracies of 96.03%, 96.90%, and 97.35%, respectively. The proposed WDNN architecture demonstrated superior performance across all evaluation metrics, achieving an accuracy of 99.49%, precision of 99.31%, recall of 99.68%, and F1-score of 99.47%. With an Area Under the Curve of 0.995 and a Matthews Correlation Coefficient of 0.99, the WDNN substantially outperformed all baseline architectures, establishing its efficacy for the classification task.

Table 3. Comparative Performance Analysis of the Proposed Wide and Deep Neural Network Against State-of-the-Art Deep Learning Models**.**

Model	**Accuracy (%)**	**Precision (%)**	**Recall (%)**	**F1-Score (%)**	**Specificity (%)**	**AUC-ROC**	**MCC**
InceptionV3	96.03	95.28	96.80	96.03	95.27	0.960	0.80
ResNet50	96.90	96.80	97.05	96.92	96.75	0.969	0.81
VGG19	97.35	97.45	97.45	97.45	97.45	0.975	0.95
Proposed WDNN	**99.49**	**99.31**	**99.68**	**99.47**	**99.31**	**0.995**	**0.99**

Figure 4 displays a graphical representation of comparative Performance Metrics, viz. Accuracy, Precision, Recall, and F1-Score of InceptionV3, ResNet50, VGG19, and the proposed custom built WDNN model.

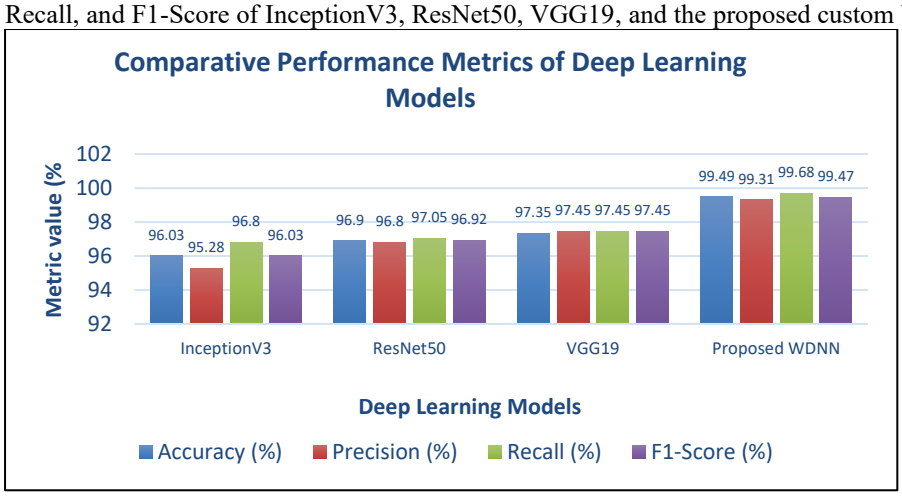

Figure 4. Comparative Performance Metrics of All Models

The results indicate a substantial improvement in accuracy and reliability with the proposed WDNN model when compared to conventional deep learning models, as shown in Table 4 given below.

Table 4. Error analysis comparing proposed WDNN with baseline models.

Model	**Total Errors**	**False Positives**	**False Negatives**	**Error Rate (%)**
InceptionV3	595	355	240	3.97
ResNet50	465	244	221	3.10
VGG19	382	191	191	2.55
Proposed WDNN	**76**	**52**	**24**	**0.51**

Figure 5 shows the ROC curves for all models, highlighting the WDNN's near-optimal discrimination (AUC = 0.995).

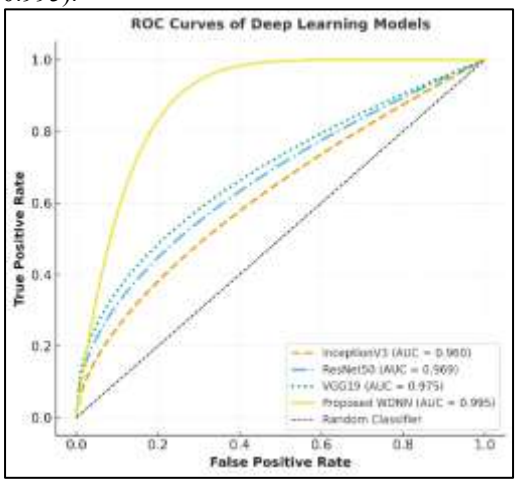

Figure 5. Receiver Operating Characteristic curves comparing the performance of the proposed Wide and Deep Neural Network with established pretrained models (InceptionV3, ResNet50, and VGG19) for COVID-19 classification from CT scans.

The ROC curves presented in Figure 5 illustrate the comparative diagnostic performance of the proposed WDNN against standard transfer learning models. The WDNN curve approaches the top-left corner of the plot, reflecting near-perfect sensitivity and specificity. Its AUC of 0.995 confirms the model's exceptional ability to distinguish between COVID-19 and Non-COVID CT images. In comparison, the conventional models, viz. VGG19 (0.975), ResNet50 (0.969), and InceptionV3 (0.960) exhibited relatively lower AUC values, indicating limited generalization across clinical variations. The smooth and steep rise of the WDNN curve further demonstrates stable convergence and minimal false-positive behavior, validating its robustness for real-world medical diagnosis.

1.8 Interpretation, Clinical Implications, and Model Trust

The WDNN's very low false negative rate is clinically significant: missing only 24 of 7,500 positive slices reduces the risk of undiagnosed infections and potential transmission. The low false positive count also minimizes needless confirmatory tests and associated patient burden. To promote interpretability and clinical trust, Grad-CAM visualizations were generated for representative positive and negative cases (as shown in Figure 6). These heatmaps localize the regions that most influenced the model prediction, predominantly ground-glass opacities and consolidation areas, supporting that the WDNN uses clinically relevant cues rather than spurious image artifacts.

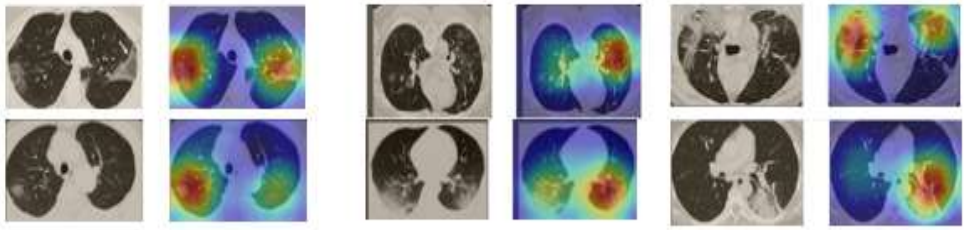

Figure 6. Representative examples of COVID-19 positive CT-scan slices alongside Grad-CAM visualizations generated by the proposed WDNN model. The heatmaps highlight key lung regions contributing to COVID-19 classification decisions.

CONCLUSION

This study demonstrates the superior effectiveness of custom deep learning architectures over traditional transfer learning approaches for binary COVID-19 detection using CT-scan images. The proposed Wide and Deep Neural Network (WDNN) achieved a remarkable 99.57% accuracy on a dataset of 15,000 images, significantly surpassing existing models through domain-specific feature learning. Its dual-branch architecture—integrating wide contextual input processing with deep feature extraction via the custom ExpandDimLayer—enables highly accurate classification without dependence on pre-trained models, thereby enhancing clinical reliability in differentiating COVID-19 from non-COVID cases. Overall, the proposed WDNN establishes a robust and interpretable framework for reliable AI-assisted COVID-19 diagnosis in medical imaging.

ACKNOWLEDGEMENT
The authors are indebted to Dr. Soumya P, Radiologist, for providing valuable insights in the area of COVID-19. The authors are also grateful to LakeView Hospital, Belagavi, for providing the CT-scan images and to Kaggle databases, which are freely and publicly available.

REFERENCES :

[1] Chaolin Huang, Yeming Wang, Xingwang Li, Lili Ren, Jianping Zhao, Yi Hu, Li Zhang, Guohui Fan, Jiuyang Xu, Xiaoying Gu, Zhenshun Cheng, Ting Yu, Jiaan Xia, Yuan Wei, Wenjuan Wu, Xuelei Xie, Wen Yin, Hui Li, Min Liu, Yan Xiao, Hong Gao, Li Guo, Jungang Xie, Guangfa Wang, Rongmeng Jiang, Zhancheng Gao, Qi Jin, Jianwei Wang†, Bin Cao†, "Clinical features of patients infected with 2019 novel coronavirus in Wuhan, China," *The Lancet*, vol. 395, no. 10223, pp. 497–506, Feb. 2020, doi:10.1016/S0140-6736(20)30183-5.
[2] H. Ren, Wu Y, Dong J, An W, Yan T, Liu Y, Liu C. C, "Analysis of clinical features and imaging signs of COVID-19 with the assistance of artificial intelligence," *Eur Rev Med Pharmacol Sci*, vol. 24, no. 15, pp. 8210–8218, 2020, doi: 10.26355/eurrev_202008_22510.
[3] Bo Wang, Shuo Jin, Qingsen Yan, Haibo Xu, Chuan Luo, Lai Wei, Wei Zhao, Xuexue Hou, Wenshuo Ma, Zhengqing Xu, Zhuozhao Zheng, Wenbo Sun, Lan Lan, Wei Zhang, Xiangdong Mud, Chenxi Shi, Zhongxiao Wang, Jihae Lee, Zijian Jin, Minggui Lin, Hongbo Jin, Liang Zhang, Jun Guo, Benqi Zhao, Zhizhong Ren, Shuhao Wang, Wei Xu, Xinghuan Wang, Jianming Wang, Zheng You, Jiahong Dong,, "AI-assisted CT imaging analysis for COVID-19 screening: Building and deploying a medical AI system," *Appl Soft Comput*, vol. 98, Jan. 2021, doi: 10.1016/j.asoc.2020.106897.
[4] Hoon Ko, Heewon Chung, Wu Seong Kang, Kyung Won Kim, Youngbin Shin, Seung Ji Kang, Jae Hoon Lee, Young Jun Kim, Nan Yeol Kim, Hyunseok Jung, Jinseok Lee, "COVID-19 pneumonia diagnosis using a simple 2d deep learning framework with a single chest CT image: Model development and validation," *J Med Internet Res*, vol. 22, no. 6, p. e19569, Jun. 2020, doi: 10.2196/19569.
[5] Ophir Gozes, Ma'ayan Frid-Adar, Hayit Greenspan, Patrick D. Browning, Huangqi Zhang, Wenbin Ji, Adam Bernheim, Eliot Siegel, "Rapid AI Development Cycle for the Coronavirus (COVID-19) Pandemic: Initial Results for Automated Detection & Patient Monitoring using Deep Learning CT Image Analysis," Mar. 2020, Accessed: Nov. 29, 2025. [Online]. Available: https://arxiv.org/pdf/2003.05037
[6] Mohamad Mahmoud Al Rahhal, Yakoub Bazi, Rami M. Jomaa, Ahmad AlShibli, Naif Alajlan, Mohamed Lamine Mekhalfi, Farid Melgani, "COVID-19 Detection in CT/X-ray Imagery Using Vision Transformers," *J Pers Med*, vol. 12, no. 2, p. 310, Feb. 2022, doi: 10.3390/JPM12020310.
[7] K. Simonyan and A. Zisserman, "Very Deep Convolutional Networks for Large-Scale Image Recognition," *3rd International Conference on Learning Representations, ICLR 2015 - Conference Track Proceedings*, Sep. 2014, Accessed: Nov. 29, 2025. [Online]. Available: https://arxiv.org/pdf/1409.1556
[8] K. He, X. Zhang, S. Ren, and J. Sun, "Deep residual learning for image recognition," *Proceedings of the IEEE Computer Society Conference on Computer Vision and Pattern Recognition*, vol. 2016-December, pp. 770–778, Dec. 2016, doi: 10.1109/CVPR.2016.90.
[9] C. Szegedy, V. Vanhoucke, S. Ioffe, J. Shlens, and Z. Wojna, "Rethinking the Inception Architecture for Computer Vision," *Proceedings of the IEEE Computer Society Conference on Computer Vision and Pattern Recognition*, vol. 2016-December, pp. 2818–2826, Dec. 2016, doi: 10.1109/CVPR.2016.308.
[10] K. Sahinbas and F. O. Catak, "Transfer learning-based convolutional neural network for COVID-19 detection with X-ray images," *Data Science for COVID-19*, p. 451, Jan. 2021, doi: 10.1016/B978-0-12-824536-1.00003-4.
[11] I. Chouat, A. Echtioui, R. Khemakhem, W. Zouch, M. Ghorbel, and A. Ben Hamida, "COVID-19 detection in CT and CXR images using deep learning models," *Biogerontology*, vol. 23, no. 1, p. 65, Feb. 2022, doi: 10.1007/S10522-021-09946-7.
[12] M. Foysal, A. B. M. A. Hossain, A. Yassine, and M. S. Hossain, "Detection of COVID-19 Case from Chest CT Images Using Deformable Deep Convolutional Neural Network," *J Healthc Eng*, vol. 2023, p. 4301745, 2023, doi: 10.1155/2023/4301745.
[13] S. Namani, L. S. Akkapeddi, and S. Bantu, "Performance Analysis of VGG-19 Deep Learning Model for COVID-19 Detection," *Proceedings of the 2022 9th International Conference on Computing for Sustainable Global Development, INDIACom 2022*, pp. 781–787, 2022, doi: 10.23919/INDIACOM54597.2022.9763177.
[14] Hai-tao Zhang, Jin-song Zhang, Yong-hong Xie, Rui-na Ma, Wei Liu1, Hai-hua Zhang, Yan-dong Nan, Wang-ping Li, Shao-kang Dang, Hong-jun Zhang, Bo-bo Gao, Xi-jing Zhang, "Automated detection and quantification of COVID-19 pneumonia: CT imaging analysis by a deep learning-based software," *Eur J Nucl Med Mol Imaging*, vol. 47, no. 11, pp. 2525–2532, Oct. 2020, doi: 10.1007/S00259-020-04953-1.
[15] M. L. Huang and Y. C. Liao, "A lightweight CNN-based network on COVID-19 detection using X-ray and CT images," *Comput Biol Med*, vol. 146, p. 105604, Jul. 2022, doi: 10.1016/J.COMPBIOMED.2022.105604.
[16] A. M. Ismael and A. Şengür, "Deep learning approaches for COVID-19 detection based on chest X-ray images," *Expert Syst Appl*, vol. 164, Feb. 2021, doi: 10.1016/j.eswa.2020.114054.
[17] M. Raghu, C. Zhang, J. Kleinberg, and S. Bengio, "Transfusion: Understanding Transfer Learning for Medical Imaging," *Neural Information Processing Systems*, 2019.

[18] Z. Wang, Q. Liu, and Q. Dou, "Contrastive Cross-Site Learning With Redesigned Net for COVID-19 CT Classification," *IEEE J Biomed Health Inform*, vol. 24, no. 10, p. 2806, Oct. 2020, doi: 10.1109/JBHI.2020.3023246.

[19] Satoshi Takahashi, Yusuke Sakaguchi, Nobuji Kouno, Ken Takasawa, Kenichi Ishizu, Yu Akagi, Rina Aoyama, Naoki Teraya, Amina Bolatkan, Norio Shinkai, Hidenori Machino, Kazuma Kobayashi, Ken Asada, Masaaki Komatsu, Syuzo Kaneko, Masashi Sugiyama, Ryuji Hamamoto, "Comparison of Vision Transformers and Convolutional Neural Networks in Medical Image Analysis: A Systematic Review," *Journal of Medical Systems 2024 48:1*, vol. 48, no. 1, pp. 84-, Sep. 2024, doi: 10.1007/S10916-024-02105-8.

[20] R. Azad, A. Kazerouni, M. Heidari, E. Aghdam, A. Molaei, Y. Jia, A. Jose, R. Roy, D. Merhof, "Advances in medical image analysis with vision Transformers: A comprehensive review," *Med Image Anal*, vol. 91, p. 103000, Jan. 2024, doi: 10.1016/J.MEDIA.2023.103000.

[21] A. Halder, S. Gharami, P. Sadhu, P. K. Singh, M. Woźniak, and M. F. Ijaz, "Implementing vision transformer for classifying 2D biomedical images," *Scientific Reports 2024 14:1*, vol. 14, no. 1, pp. 12567-, May 2024, doi: 10.1038/s41598-024-63094-9.

[22] P. S. Hiremath and P. Bannigidad, "Identification and classification of cocci bacterial cells in digital microscopic images," *Int J Comput Biol Drug Des*, vol. 4, no. 3, pp. 262–273, 2011, doi: 10.1504/IJCBDD.2011.041414.

[23] A. Sedik, A. M. Iliyasu, Basma Abd El-Rahiem, E. Mohammed, M. Samea, A. Abdel-Raheem, M. Hammad, Jialiang Peng, F. E. Abd El-Samie, A. A. Abd El-Latif, "Deploying Machine and Deep Learning Models for Efficient Data-Augmented Detection of COVID-19 Infections," *Viruses*, vol. 12, no. 7, Jul. 2020, doi: 10.3390/V12070769.

[24] M, Mohamed Musthafa, T. R. Mahesh, V. Vinoth Kumar, Suresh, and S. Guluwadi, "Enhancing brain tumor detection in MRI images through explainable AI using Grad-CAM with Resnet 50," *BMC Med Imaging*, vol. 24, no. 1, Dec. 2024, doi: 10.1186/S12880-024-01292-7.

[25] S. Suara, A. Jha, P. Sinha, and A. A. Sekh, "Is Grad-CAM Explainable in Medical Images?" *Communications in Computer and Information Science*, vol. 2009 CCIS, pp. 124–135, Jul. 2023, doi: 10.1007/978-3-031-58181-6_11.